($kh_2 = 1.33$), 54 percent ($kh_2 = 1.50$), 14 percent ($kh_2 = 2.00$) to zero.

Configuration C (Fig. 4)

For this configuration no enhancement is found.

Configuration D (Fig. 5)

Curve $kh_1 = 0.5$: a small enhancement of about 2 percent is present in the range $kh_2 = 0.38$ to 0.5.

ACKNOWLEDGMENT

The authors wish to thank Prof. S. Middelhoek and Dr. G. de Jong for valuable discussions.

REFERENCES

[1] F. S. Hickernell, "The role of layered structures in surface acoustic wave technology," in *1973 Proc. IEEE Conf. Component Performance and Systems Applications of Surface Acoustic Wave Devices* (Aviemore, Scotland, 1973), pp. 11–21, Conf. Publ. 109.

[2] J. J. Campbell and W. R. Jones, "A method for estimating optimal crystal cuts and propagation directions for excitation of piezoelectric surface waves," *IEEE Trans. Sonics Ultrason.*, vol. SU-15, pp. 209–217, Oct. 1968.

[3] G. W. Farnell and E. L. Adler, "Elastic wave propagation in thin layers," in *Physical Acoustics*, vol. 9, W. P. Mason, Ed. New York: Academic, 1972.

[4] G. A. Armstrong and S. Crampin, "Piezoelectric surface wave calculations in multilayered anisotropic media," *Electron. Lett.*, vol. 8, pp. 521–522, 1972.

[5] A. H. Fahmy and E. L. Adler, "Propagation of acoustic surface waves in multilayers: A matrix description," *Appl. Phys. Lett.*, vol. 22, pp. 495–497, May 1973.

[6] A. J. Slobodnik and E. D. Conway, "Surface wave velocities," in *Microwave Acoustics Handbook*, USAF Res. Lab., Cambridge, Mass., Rep. AFCRL-70-0164, 1970.

[7] B. A. Auld, *Acoustic Fields and Waves in Solids*, vol. 1. New York: Wiley, 1973.

[8] L. P. Solie, "Piezoelectric wave on layered substrates," *J. Appl. Phys.*, vol. 44, pp. 619–627, Feb. 1973.

Microwave Propagation in Rectangular Waveguide Containing a Semiconductor Subject to a Transverse Magnetic Field

J. B. NESS AND M. W. GUNN

Abstract—**The propagation constant of waveguide partially loaded with a semiconductor in the *H* plane is evaluated using a three-mode approximation analysis. As the waveguide is progressively filled, a large peak occurs in the attenuation coefficient due to higher order mode propagation. In the presence of a transverse magnetic field, propagation becomes nonreciprocal and this nonreciprocal effect is shown to be significantly increased in the region of the peak. The theoretical results are verified using n-type germanium samples in 26.5–40-GHz waveguide.**

INTRODUCTION

The propagation characteristics of rectangular waveguide loaded with dielectric or semiconductor slabs have been investigated by many researchers [1]–[4], and these characteristics have been used to measure material properties or as a basis for construction of microwave devices. Semiconductor loading presents a more difficult problem for analysis than lossless dielectric, and if the semiconductor material is anisotropic, as occurs in the presence of a magnetic field, the problem is further complicated.

Waveguide partially loaded with a semiconductor subject to a transverse magnetic field may exhibit nonreciprocal propagation, and the possibility exists of constructing isolators, circulators, variable attenuators, etc., using semiconductor-loaded waveguide. Such nonreciprocal propagation has been studied experimentally [5], [6], and approximate theoretical analyses for both reciprocal and nonreciprocal propagation have been given by several authors [7]–[9]. Experimental devices such as isolators and power dividers have also been constructed [5], [10].

An approximation technique due to Schelkunoff [11] was used by Arnold and Rosenbaum [12] to analyze the partially loaded waveguide shown in Fig. 1. An approximate solution for the propagation constant was obtained using a two-mode (TE_{10} and TM_{11}) analysis, and was shown to give reasonable agreement with experimental results.

In this short paper, a three-mode (TE_{10}, TE_{11}, TM_{11}) analysis is used, and although the mathematics becomes more complex, an improvement in accuracy is evident and certain aspects of the propagation constant are illustrated more clearly.

THEORY

For a semiconductor subject to a transverse magnetic field, as shown in Fig. 1, the permittivity becomes a tensor given by [7], [12].

$$[\epsilon] = \begin{bmatrix} \epsilon_{11} & 0 & 0 \\ 0 & \epsilon_{22} & \epsilon_{23} \\ 0 & \epsilon_{32} & \epsilon_{33} \end{bmatrix}$$

$$\epsilon_{11} = \epsilon_0\epsilon_r\left[1 - \frac{j\sigma}{\omega\epsilon_0\epsilon_r}\right]$$

$$\epsilon_{22} = \epsilon_{33} = \epsilon_0\epsilon_r\left[1 - \frac{j\sigma}{\omega\epsilon_0\epsilon_r[1 + (R_cB_0\sigma)^2]}\right]$$

$$\epsilon_{23} = -\epsilon_{32} = \frac{jR_cB_0\sigma^2}{\omega[1 + (R_cB_0\sigma)^2]}$$

where

- R_c Hall coefficient;
- σ dc conductivity;
- B_0 magnetic-field strength;
- ϵ_r relative permittivity.

The simplifying assumptions that only one type of carrier is present and that the signal frequency ω is much less than the scattering frequency so that σ is essentially constant, are used in the preceding equations. Thus the semiconductor parameters and the magnetic field enter the problem through the tensor permittivity.

For the two-mode approximation, the method of obtaining the propagation constant is given by Arnold and Rosenbaum [12] and the three-mode analysis is similar except that a sixth-order polynomial in γ, the propagation coefficient, is obtained, i.e.,

$$\gamma^6 + A_5\gamma^5 + A_4\gamma^4 + A_3\gamma^3 + A_2\gamma^2 + A_1\gamma + A_0 = 0 \qquad (1)$$

where all A_n are in general complex. The analytical forms of the coefficients $A_0, \cdots, A_5$ are given in the Appendix.

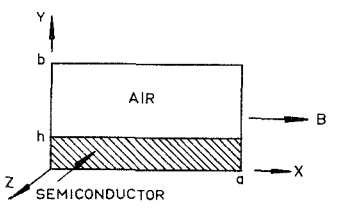

Fig. 1. Partially filled rectangular guide.

Manuscript received November 13, 1974; revised May 5, 1975. This work was supported in part by the Australian Research Grants Committee and the Australian Radio Research Board.

The authors are with the Department of Electrical Engineering, University of Queensland, Brisbane, Qld., Australia.

Equation (1) was solved using a numerical computer program which works in double precision.

For the reciprocal case, that is, when the propagation coefficient is the same in both the forward and reverse directions, the coefficients of the odd terms A_5, A_3, and A_1 are zero and three different roots are obtained, but in general the solution of (1) has six different roots. The roots selected for the forward and reverse propagation coefficients are the ones with the smallest values of attenuation coefficient. In most cases, one set of roots will have an attenuation coefficient an order of magnitude less than the other sets. This is considered essentially single-mode propagation. If the real parts of the roots, that is, the attenuation coefficients, are of approximately equal magnitude, propagation is considered to be multimode. In this case, the phase coefficients are usually quite different and so the modes can be readily distinguished on a theoretical basis.

The modes selected for the analysis are usually those with the lowest cutoff frequencies in the empty guide. However, for the case shown in Fig. 1, a three-mode analysis using the TE_{10}, TE_{01}, and TM_{11} modes gave the same results as the two-mode analysis, indicating that the TE_{01} mode was not coupled to the other two. Although the effect of a mode on the propagation would be expected to decrease as the order of the mode increases, this is not always the case. The TE_{11} mode, for example, has a much greater influence on the propagation than the lower order TE_{01} mode. The importance of the TE_{11} mode is expected since it is degenerate with the TM_{11} mode in empty waveguide. The particular modes selected will depend on the structural details of the loaded waveguide. For a centrally placed E-plane slab, the three-mode analysis using the TE_{10}, TE_{20}, and TM_{11} modes gives better results than the TE_{10}, TE_{11}, and TM_{11}-mode analysis. Thus to obtain reasonable accuracy and avoid the complexity of four- or five-mode analyses, it is important to choose the set of basis modes carefully.

RESULTS

The attenuation coefficient as a function of filling ratio h/b for the structure of Fig. 1 is shown in Fig. 2. The two-mode and three-mode theoretical results are compared with the experimental results obtained by Arnold and Rosenbaum using n-type silicon (σ = 10 S/m) in X-band waveguide. The three-mode analysis is seen to give better agreement with the experimental results than the two-mode analysis. Fig. 3 shows the variation of attenuation coefficient with frequency for the partially filled guide. The three-mode analysis gives results agreeing very closely with the experimental results of Arnold and Rosenbaum.

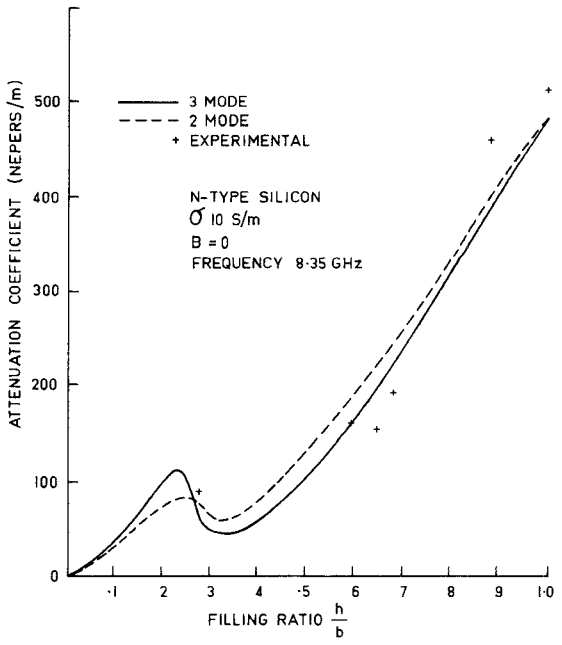

Fig. 2. Attenuation coefficient as a function of filling ratio at X band.

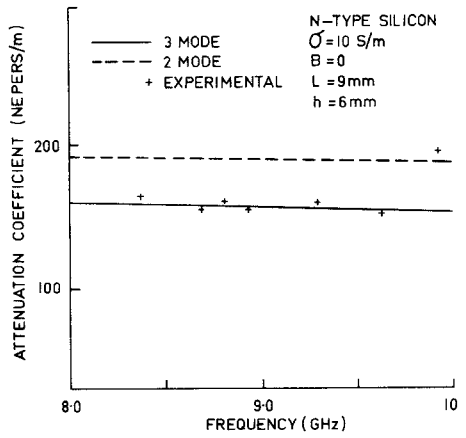

Fig. 3. Variation of attenuation coefficient with frequency for the partially filled guide.

The peak in the attenuation coefficient shown in Fig. 2 is more pronounced for the three-mode analysis. This peak has been discussed by Gardiol and Parriaux [13] and, for the case of zero magnetic field, is due to a change in propagation from the LSM_{11} mode to the LSM_{21} mode.

The three-mode analysis has been applied to the loading shown in Fig. 1 using n-type germanium (σ = 12.0 S/m) in Q-band waveguide (7.112 by 3.556 mm). Fig. 4 shows the variation of attenuation coefficient with filling ratio h/b for the loaded waveguide at a frequency of 30 GHz and with a transverse magnetic flux density of 2.0 T. The experimental peak is narrower and of smaller magnitude than the theoretical peak and also occurs at a lower value of h/b. Theoretical results for the two-mode analysis have also been included in Fig. 4, and it is readily seen that the three-mode analysis gives better results. The theoretical and experimental curves show similar crossover points for the forward and reverse traveling waves, and that the peak for the reverse wave is higher and occurs at a slightly lower value of h/b than the forward wave peak. Fig. 5 shows the variation of the phase coefficient with the filling ratio h/b. A similar peak exists in the phase coefficient but occurs at a slightly lower value of h/b in both the theoretical and experimental results than the peak in the attenuation coefficient. However, the phase coefficient peak is not as pronounced as the attenuation peak and the difference between the phase coefficients of the forward and reverse waves is only small. The reverse wave, that is, the wave traveling in the $-z$ direction is obtained experimentally by simply reversing the direction of the applied magnetic field.

A microwave transmission bridge was used to measure the attenuation and to preserve phase information; the semiconductor loaded waveguide was not matched. When losses due to reflection or transmission are high, the bridge becomes insensitive to phase. Thus the accuracy of the phase measurements deteriorates as the attenuation increases. The experimental results were obtained using three similar samples of different lengths (2.68, 1.81, and 1.26 cm), and the attenuation coefficient was estimated from the slope of the attenuation versus length curve for the three samples. This should give a reasonably accurate value of attenuation coefficient as the sample lengths are all longer than the guide wavelength. The phase coefficient was estimated in a similar fashion. For low values of h/b (<0.2), the reflected power is very small but both reflected and absorbed power increase rapidly for higher values of h/b making it difficult to measure the attenuation for $h/b > 0.7$.

The discrepancy between the theory and the experimental results is due in part to the finite number of modes used in the analysis. The choice of modes also affects the accuracy of the analysis. For low values of h/b (<0.2), the analysis method is more accurate if the TE_{10}, TE_{20}, and TM_{11} modes are used. However, for $h/b > 0.2$ better agreement with the experimental results is obtained if the TE_{10}, TE_{11}, and TM_{11} modes are selected. This indicates that to obtain accurate results over the whole range of h/b, a higher number of modes will be required for the analysis.

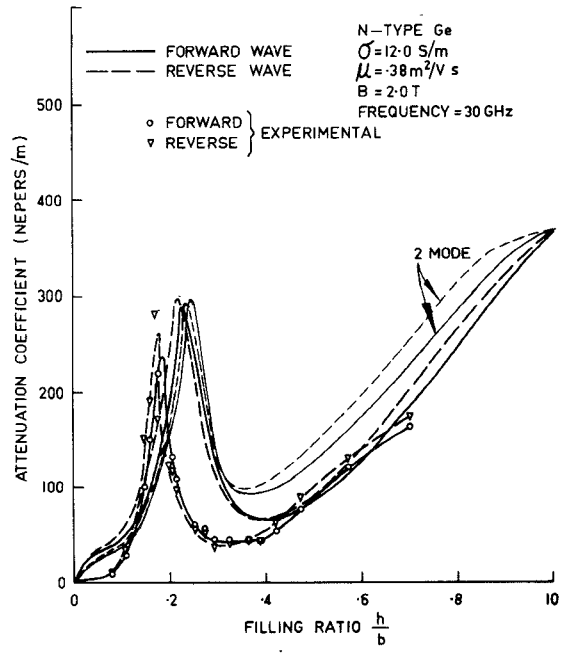

Fig. 4. Attenuation coefficient as a function of filling ratio at 30 GHz.

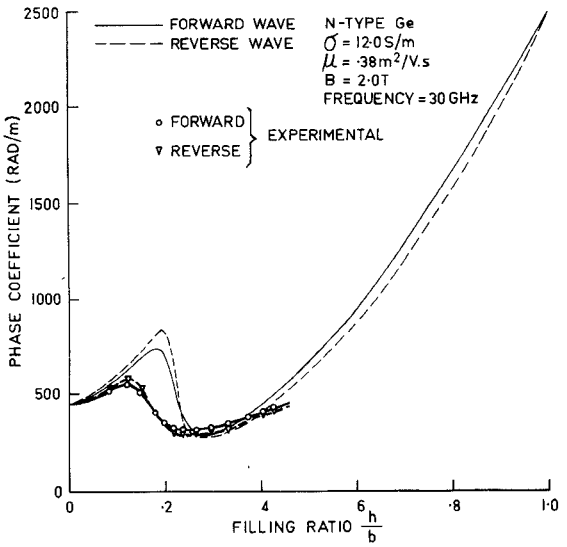

Fig. 5. Phase coefficient as a function of filling ratio at 30 GHz.

The experimental values of the attenuation coefficient may be somewhat lower than the actual values due to a very slight air gap between the sample and the bottom of the waveguide. The air gap between the sample and the narrow walls of the waveguide was very small (all samples were 7.1 mm wide) and has negligible effect. Somlo [14] has shown that an air gap between the sample and the bottom of the waveguide can lead to a significant drop in the measured attenuation. The effect of this air gap can be estimated by considering the case when the magnetic field is zero. In this case, propagation is either by the LSM_{11} or LSM_{21} mode and exact solutions for the propagation coefficient as a function of h/b can be obtained. When the experimental results were compared to the exact solutions, the attenuation coefficient was found to be accurate within 5 percent and the phase coefficient was accurate to 3 percent for nearly all values of h/b. The air gap is difficult to eliminate because of the slight rounding of the internal corners of the waveguide. The bottom corners of the samples were also slightly rounded but this did not completely eliminate the air gap due to the slight variations in width along the waveguide. To obtain experimental results over a wide range of h/b, the samples were removed from the guide after each measurement and then lapped to the required height before inserting in the waveguide. To avoid chipping or cracking in this process, a really tight fit of the sample in the guide must be avoided so an air gap is inevitable. The measurements were independent of the longitudinal position of the sample as long as the sample was kept in the uniform magnetic-field region.

Theoretically, the peak should shift towards lower values of h/b as the frequency is increased, and this has been verified experimentally although the shift is only slight. For the germanium sample used, a frequency change from 30 to 34 GHz causes the theoretical peak to shift from $h/b = 0.22$ to 0.20 whereas the experimental peak shifts from $h/b = 0.175$ to 0.165.

The effect of the magnetic field on the attenuation coefficient depends on the filling ratio h/b. Fig. 6 shows the variation of measured attenuation with magnetic flux density for two values of h/b on either side of the experimental peak. As expected theoretically, the variation of attenuation with magnetic flux density is relatively small away from the peak and the nonreciprocity is also small. The dependency of the attenuation on the magnetic field increases sharply as the value of h/b becomes closer to the value at the peak. This is shown in Fig. 7 where the values of h/b are very close to the value at the peak (0.175 at 30 GHz). Moreover, the attenuation increases with magnetic field for both directions of propagation and the nonreciprocity is also greater very close to the peak (about 15 dB at 2.0 T for $h/b = 0.167$).

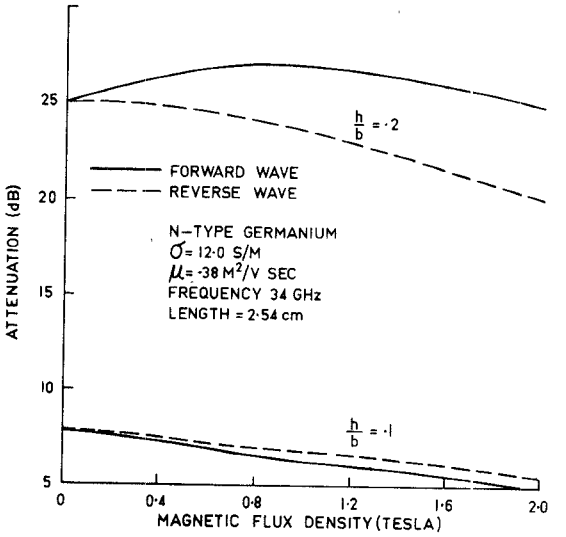

Fig. 6. Measured change in attenuation with magnetic field away from the peak.

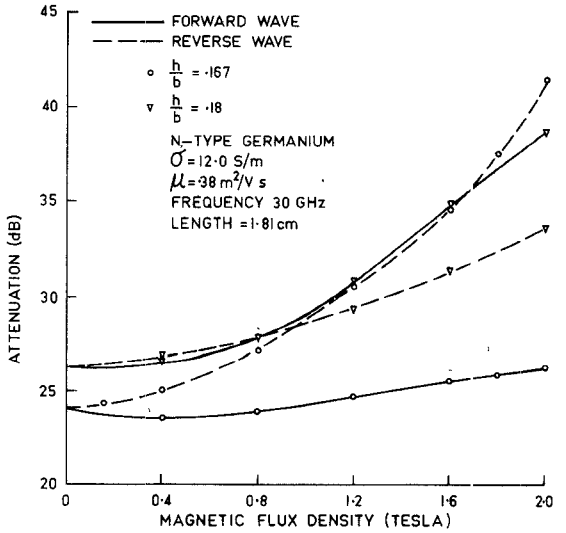

Fig. 7. Measured change in attenuation with magnetic field very close to the peak.

Theoretically, the nonreciprocity was found to be a maximum just on either side of the peak. In this region, the TM_{11}-like mode propagates with an attenuation coefficient approximately equal to that of the distorted TE_{10} mode. Hence the E_z component of the electric field contributed by the TM_{11} mode should be a maximum in this region, and thus the nonreciprocity should be a maximum. The measured nonreciprocity was found to be greatest just before the peak, that is, just before higher order mode propagation occurs.

DISCUSSION

The peak in the attenuation coefficient is caused by the change in propagation from one mode to another. This can be seen more clearly from Fig. 8 where the roots for the forward wave (i.e., the roots of (1) with positive real parts) are shown as a function of h/b. For low values of h/b (<0.1), the propagation mode is a quasi-TE_{10} mode (the LSM_{11} mode for zero magnetic field). In the region of the peak where multimode propagation occurs, the main mode of propagation changes from a TE_{10}-like mode to a TE_{11}-like mode. As h/b increases further, propagation is essentially single mode until, as h/b approaches unity, the roots tend toward a common value, perhaps indicating an anomalous mode with all components of the three modes [7]. For the fully filled guide the propagation mode is TE_{10} for zero magnetic field but, as seen from Fig. 8, this is no longer the case when a magnetic field is applied.

The position of the peak, its magnitude, and the nonreciprocity depend on the semiconductor parameters as well as the magnetic field and the frequency. In general, increasing the conductivity or the permittivity shifts the peak towards smaller values of h/b and increasing the frequency has a similar effect. The nonreciprocity will increase if the magnitude of the off diagonal terms in the tensor permittivity is increased relative to the diagonal terms. This may be achieved theoretically by lowering the dielectric constant to effectively reduce the diagonal terms. For example, for a sample of conductivity 12.0 S/m and at a frequency of 30 GHz, the theoretical nonreciprocity is increased about eight times if the dielectric constant is decreased from 16.0 to 4.0. Increasing the mobility will also increase the nonreciprocity. However, for H-plane loading it was found that high mobility n-type InSb samples had a much smaller nonreciprocity than the n-type Ge samples. This was due to the fields being excluded from the InSb because of the high conductivity ($\sigma = 2.0 \times 10^4$ S/m). Since a semiconductor with low conductivity, low dielectric constant, and high mobility is not available, it is difficult to achieve reasonable nonreciprocity without high insertion loss for bulk semiconductor loading in the H plane. It may be possible, however, to achieve low insertion loss and high nonreciprocity by mounting a semiconducting film on a lossless dielectric of suitable height and permittivity [15].

Other theoretical results for waveguide partially filled with a semiconductor in the presence of a transverse magnetic field do not appear to be available in the literature. However, Fig. 9 compares the results obtained from the three-mode analysis with that obtained by Gunn and Rahmann [16]. The agreement between the two methods is very close except that for higher values of magnetic field the results diverge slightly. In the absence of a magnetic field, this analysis gives very accurate results for the propagation constant in the fully filled guide for any values of conductivity or permittivity. However, for the partially filled guide the accuracy of the three-mode analysis deteriorates as the conductivity and permittivity increase. For $\sigma = 2.0$ S/m and $\epsilon_r = 12.0$, good agreement is found between the exact solution [13] and the three-mode approximation for all values of h/b in X-band waveguide. However, for $\sigma > 20$ S/m quantitative agreement is poor although the peak position is very close to that given by the exact analysis.

CONCLUSION

The three-mode analysis has been applied to the H-plane loading geometry shown in Fig. 1, and gives more accurate results than the two-mode analysis. This analysis also shows explicitly the peak in the attenuation coefficient as the waveguide is progressively filled. Theoretically, the nonreciprocity was found to be a maximum in the region of the peak, and this has been verified experimentally. Although the accuracy of this method is not good for higher conductivities (>20 S/m), the method is still useful for estimating the position of the peak and the start of higher mode propagation. The

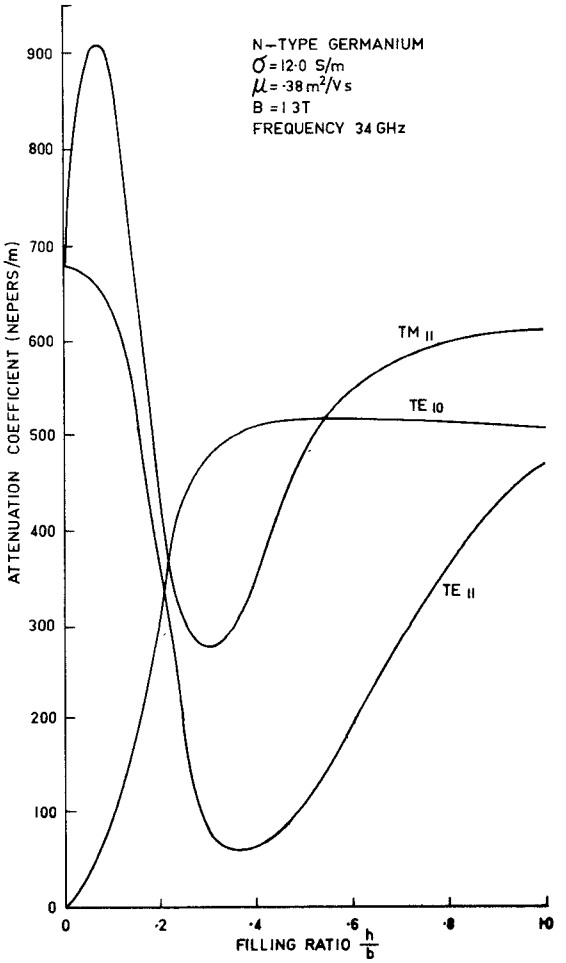

Fig. 8. Attenuation coefficient for each mode as a function of filling ratio.

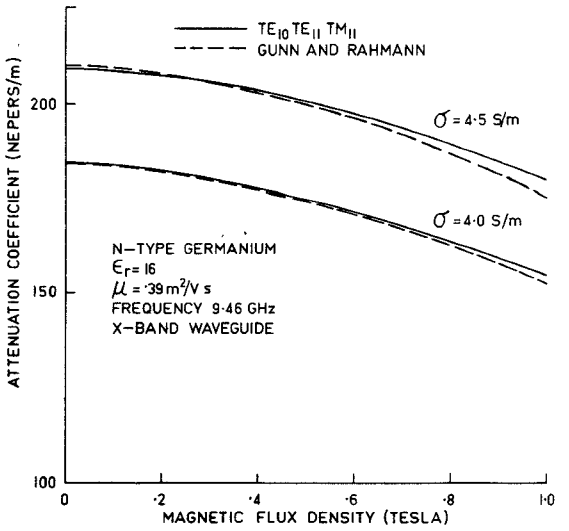

Fig. 9. Theoretical variation of attenuation coefficient with magnetic field for the fully filled guide.

accuracy of the three-mode analysis can be improved by a different choice of modes for certain loadings, but to achieve better accuracy over the whole range of h/b, a higher number of modes would be required.

The experimental results indicate that nonreciprocity suitable for practical devices can be achieved using H-plane loading. However, the insertion loss caused by using this configuration is too high for device purposes. A method of reducing the insertion loss by using a thin film of semiconductor placed on a low-loss high dielectric substrate has been proposed by Gardiol [15]. The H-plane dielectric slab sets up the circularly polarized electric field, and the semiconductor material can then be positioned on top of the dielectric slab for optimum nonreciprocity. However, no experimental results have been published as yet. E-plane InSb isolators, which are comparable to ferrite isolators, have been constructed [5] for the 75–110-GHz frequency band except that much higher magnetic fields are required. Similar devices operating at lower frequencies [9], [10] have not been as successful. The H-plane structure offers the possibility of achieving useful nonreciprocity at the lower as well as the upper millimeter range. The reduction of the insertion loss by the previously outlined method, as well as a more suitable choice of semiconductor material, may enable useful devices to be constructed.

APPENDIX

When three modes are selected for the analysis, the coefficients of the complex polynomial are obtained from a sixth-order determinant. The development of this determinant is similar to that given in [12] so only the results will be given here.

For the $TE_{[10]}$, $TE_{[11]}$, and $TM_{(11)}$ modes, the following matrix equation of order 6 is obtained:

$$\begin{bmatrix} E+\gamma & D & L & F & 0 & 0 \\ 0 & \gamma & 0 & 0 & G & 0 \\ 0 & 0 & \gamma & 0 & 0 & G \\ B & A & K & C+\gamma & 0 & 0 \\ I & H & M & J & \gamma & 0 \\ N & R & P & Q & 0 & \gamma \end{bmatrix} \begin{bmatrix} V_{(11)} \\ V_{[10]} \\ V_{[11]} \\ I_{(11)} \\ I_{[10]} \\ I_{[11]} \end{bmatrix} = [0]. \quad \text{(A1)}$$

By equating the determinant of this matrix to zero, the coefficients of the sixth-order polynomial are obtained as follows:

$$A_5 = C + E$$

$$A_4 = CE - BF - GP - GH$$

$$A_3 = G(IN + QK + DI + AJ - EP - CP - EH - CH)$$

$$A_2 = G(CLN + QER + CDI + AEJ + GHP + BFH + BFP - BLQ - CEP - BDJ - CEH - GMR - FKN - AFI)$$

$$A_4 = G^2(DMN + ILR + EHP + CHP + AMQ + JKP - DIP - HLN - HKQ - EMR - CMR - AJP)$$

$$A_0 = G^2(CDMN + DIKQ + BDJP + BHLQ + CILR + AJLN + AEMQ + CEHP + FHKN + BFMR + AFIP + EJKR - BDMQ - CDIP - CHLN - AILQ - DKJN - BJLR - EHKQ - CEMR - AEJP - BFHP - AFMN - FIKR)$$

where

$$A = -\left(K12 + \frac{K3.K15}{K1}\right)$$

$$B = -\left(K10 + K11 - \frac{K2.K15}{K1}\right)$$

$$C = \frac{K15}{K1}$$

$$D = \frac{K3}{K1}\chi_{(11)}$$

$$E = \frac{-K2}{K1}\chi_{(11)}$$

$$F = -\left(K5 + K6 + \frac{\chi_{(11)}}{K1}\right)$$

$$G = -K7$$

$$H = -\left(K16 + \frac{\chi_{[10]}}{K8} - \frac{K3K17}{K4}\right)$$

$$I = -\left(K12 + \frac{K2.K17}{K1}\right)$$

$$J = \frac{-K17}{K1}$$

$$K = K13 - K14 - \frac{K15.K4}{K1}$$

$$L = \frac{K4\chi_{(11)}}{K1}$$

$$M = -\left(\frac{b}{a}K12 - \frac{K17K4}{K1}\right)$$

$$N = \left(\frac{a}{b}K10 - \frac{b}{a}K11 - \frac{K2K18}{K1}\right)$$

$$P = -\left(\frac{a}{b}K10 + \frac{b}{a}K11 - \frac{K4.K18}{K1} + \frac{\chi_{(11)}}{K9}\right)$$

$$Q = \frac{-K18}{K1}$$

$$R = -\left(\frac{b}{a}K12 - \frac{K3.K18}{K1}\right)$$

and

$$K1 = \frac{j\omega\chi_{(11)}a^2b}{\pi^2(a^2+b^2)}\left[\epsilon_0\left(b - h + \frac{b}{2\pi}\sin\frac{2\pi h}{b}\right) + \epsilon_{22}\left(h - \frac{b}{2\pi}\sin\frac{2\pi h}{b}\right)\right]$$

$$K2 = \frac{j\omega a^2b}{2\pi^2(a^2+b^2)}\epsilon_{32}\left(1 - \cos\frac{2\pi h}{b}\right)$$

$$K3 = \frac{j\omega}{\pi^2}\frac{ab\sqrt{2}}{(a^2+b^2)^{1/2}}\epsilon_{32}\left(\cos\frac{\pi h}{b} - 1\right)$$

$$K4 = \frac{j\omega ab^2}{2\pi^2(a^2+b^2)}\epsilon_{32}\left(\cos\frac{2\pi h}{b} - 1\right)$$

$$K5 = \frac{j\omega\mu_0a^2}{a^2+b^2}$$

$$K6 = \frac{j\omega\mu_0b^2}{a^2+b^2}$$

$$K7 = j\omega\mu_0$$

$$K8 = j\omega\mu_0 \frac{a}{\pi}$$

$$K9 = \frac{j\omega\mu_0\chi_{[11]}a^2b^2}{\pi^2(a^2+b^2)}$$

$$K10 = \frac{j\omega b}{a^2+b^2}\left[\epsilon_0\left(b-h+\frac{b}{2\pi}\sin\frac{2\pi h}{b}\right)+\epsilon_{11}\left(h-\frac{b}{2\pi}\sin\frac{2\pi h}{b}\right)\right]$$

$$K11 = \frac{j\omega a^2}{b(a^2+b^2)}\left[\epsilon_0\left(b-h-\frac{b}{2\pi}\sin\frac{2\pi h}{b}\right)+\epsilon_{22}\left(h+\frac{b}{2\pi}\sin\frac{2\pi h}{b}\right)\right]$$

$$K12 = \frac{j\omega a\sqrt{2}}{\pi(a^2+b^2)^{1/2}}(\epsilon_{22}-\epsilon_0)\sin\frac{\pi h}{b}$$

$$K13 = \frac{a}{b}K10$$

$$K14 = \frac{b}{a}K11$$

$$K15 = \frac{j\omega\chi_{(11)}a^2b}{2\pi^2(a^2+b^2)}\epsilon_{23}\left(1-\cos\frac{2\pi h}{b}\right)$$

$$K16 = \frac{j\omega}{b}[\epsilon_0(b-h)+\epsilon_{22}h]$$

$$K17 = \frac{j\omega\chi_{(11)}ab\sqrt{2}}{\pi^2(a^2+b^2)^{1/2}}\epsilon_{23}\left(\cos\frac{\pi h}{b}-1\right)$$

$$K18 = \frac{j\omega\chi_{(11)}ab^2}{2\pi^2(a^2+b^2)}\epsilon_{23}\left(\cos\frac{2\pi h}{b}-1\right)$$

$$\chi_{[11]} = \chi_{(11)} = \left(\frac{\pi^2}{a^2}+\frac{\pi^2}{b^2}\right)^{1/2}.$$

For more than three modes, this method of obtaining γ becomes too inefficient. For four or more modes, that is, in cases where a matrix of order 8 or higher is obtained, the propagation coefficient could be evaluated by finding the eigenvalues of the complex matrix.

REFERENCES

[1] F. E. Gardiol, "Higher-order modes in dielectrically loaded rectangular waveguides," *IEEE Trans. Microwave Theory Tech.*, vol. MTT-16, pp. 919–924, Nov. 1968.

[2] Y. Mushiake and T. Ishida, "Characteristics of loaded rectangular waveguides," *IEEE Trans. Microwave Theory Tech.*, vol. MTT-13, pp. 451–457, July 1965.

[3] R. H. Sheikh and M. W. Gunn, "Wave propagation in rectangular waveguide inhomogeneously filled with semiconductors," *IEEE Trans. Microwave Theory Tech.* (Corresp.), vol. MTT-16, pp. 117–121, Feb. 1968.

[4] A. N. Datta and B. R. Nag, "Techniques for the measurement of complex microwave conductivity and the associated error," *IEEE Trans. Microwave Theory Tech.*, vol. MTT-18, pp. 162–166, Mar. 1970.

[5] K. Suzuki and R. Hirota, "Nonreciprocal millimeter-wave devices using a solid-state plasma at room temperature," *IEEE Trans. Electron Devices*, vol. ED-18, pp. 408–411, July 1971.

[6] H. E. Barlow and R. Koike, "Microwave propagation in a waveguide containing a semiconductor to which is applied a steady transverse magnetic field," *Proc. Inst. Elec. Eng.*, vol. 110, pp. 2177–2181, 1963.

[7] M. H. Engineer and B. R. Nag, "Propagation of electromagnetic waves in rectangular guides filled with a semiconductor in the presence of a transverse magnetic field," *IEEE Trans. Microwave Theory Tech. (Special Issue on Microwave Filters)*, vol. MTT-13, pp. 641–646, Sept. 1965.

[8] G. J. Gabriel and M. E. Brodwin, "Perturbation analysis of rectangular waveguide containing transversely magnetized semiconductor," *IEEE Trans. Microwave Theory Tech.*, vol. MTT-14, pp. 258–264, June 1966.

[9] R. Hirota and K. Suzuki, "Field distribution in a magnetoplasma-loaded waveguide at room temperature," *IEEE Trans. Microwave Theory Tech.*, vol. MTT-18, pp. 188–195, Apr. 1970.

[10] R. J. Dinger and D. J. White, "The use of a thin vacuum-deposited InSb film as a *K*-band field displacement isolator," *Proc. IEEE* (Lett.), pp. 646–647, May 1972.

[11] S. A. Schelkunoff, "Generalized telegraphists equations for waveguides," *Bell Syst. Tech. J.*, pp. 784–801, July 1952.

[12] R. M. Arnold and F. J. Rosenbaum, "Nonreciprocal wave propagation in semiconductor loaded waveguides in the presence of a transverse magnetic field," *IEEE Trans. Microwave Theory Tech.*, vol. MTT-19, pp. 57–65, Jan. 1971.

[13] F. E. Gardiol and O. Parriaux, "Excess losses in *H*-plane loaded waveguides," *IEEE Trans. Microwave Theory Tech.*, vol. MTT-21, pp. 457–461, July 1973.

[14] P. I. Somlo, "The exact numerical evaluation of the complex dielectric constant of a dielectric partially filling a waveguide," *IEEE Trans. Microwave Theory Tech.* (Lett.), vol. MTT-22, pp. 468–469, Apr. 1974.

[15] F. E. Gardiol, "Circularly polarized electric field in rectangular waveguide," *IEEE Trans. Microwave Theory Tech.* (Short Papers), vol. MTT-22, pp. 563–565, May 1974.

[16] M. W. Gunn and S. A. Rahmann, "Effect of the Hall field in a rectangular waveguide containing semiconducting material," *Proc. Inst. Elec. Eng.*, vol. 117, pp. 2238–2240, Dec. 1970.

Letters

Transmission Line Transformation Between Arbitrary Impedances Using the Smith Chart

P. I. DAY

***Abstract*—A graphical method for transforming between two complex impedances using a single transmission line matching section is described. The Smith chart is used in a mode where the chart normalizing impedance is arbitrary.**

In a recent letter, Arnold [1] presented a graphical method for transforming complex load impedances into resistive load impedances using a transmission line section, determining both the line impedance and length. The Smith chart was used although the line impedance was initially unknown. The method can be extended to cover the transformation between two complex impedances using a construction described in earlier literature for evaluating the line impedance in the complex transformation.

Somlo [2] showed that the characteristic impedance required for a line to transform two arbitrary impedances can be found by using an arbitrary normalizing impedance and constructing a circle centered on the real axis passing through the two impedance points. The technique was based on these properties of a Smith chart: 1) the locus of impedance along a loss-free line is always a circle; 2) the line impedance is given by the geometric mean of the circle intercepts with the real axis. A further property not mentioned by Somlo is that: 3) the square root of the ratio of the intercepts is the VSWR on the line.

The line length could be determined by reentering the Smith chart in the normal manner with the calculated line impedance. This letter

Manuscript received February 18, 1975; revised April 28, 1975.

The author is with the Department of Engineering, Cambridge University, Cambridge, England.